

Heterogeneous distribution of viscosupplements *in vivo* is correlated to *ex vivo* frictional properties of equine cartilage

Karan Vishwanath¹  | Scott R. McClure² | Lawrence J. Bonassar^{3,4}

¹Department of Materials Science and Engineering, Cornell University, Ithaca, New York, USA

²Midwest Equine Surgery and Sport Medicine, Boone, Iowa, USA

³Meinig School of Biomedical Engineering, Cornell University, Ithaca, New York, USA

⁴Sibley School of Mechanical and Aerospace Engineering, Cornell University, Ithaca, New York, USA

Correspondence

Lawrence J. Bonassar, Meinig School of Biomedical Engineering, Sibley School of Mechanical and Aerospace Engineering, 149 Weill Hall, Cornell University, Ithaca, NY 14853, USA.
 Email: lb244@cornell.edu

Funding information

Cornell Center for Materials Research, Grant/Award Number: DMR1719875; National Institute of Health, Grant/Award Number: S10OD025049; National Science Foundation LEAP-HI CMMI, Grant/Award Number: 2245367

Abstract

Intra-articular injections of hyaluronic acid (HA) are the cornerstone of osteoarthritis (OA) treatments. However, the mechanism of action and efficacy of HA viscosupplementation are debated. As such, there has been recent interest in developing synthetic viscosupplements. Recently, a synthetic 4 wt% polyacrylamide (pAAm) hydrogel was shown to effectively lubricate and bind to the surface of cartilage *in vitro*. However, its ability to localize to cartilage and alter the tribological properties of the tissue in a live articulating large animal joint is not known. The goal of this study was to quantify the distribution and extent of localization of pAAm in the equine metacarpophalangeal or metatarsophalangeal joint (fetlock joint), and determine whether preferential localization of pAAm influences the tribological properties of the tissue. An established planar fluorescence imaging technique was used to visualize and quantify the distribution of fluorescently labeled pAAm within the joint. While the pAAm hydrogel was present on all surfaces, it was not uniformly distributed, with more material present near the site of the injection. The lubricating ability of the cartilage in the joint was then assessed using a custom tribometer across two orders of magnitude of sliding speed in healthy synovial fluid. Cartilage regions with a greater coverage of pAAm, that is, higher fluorescent intensities, exhibited friction coefficients nearly 2-fold lower than regions with lesser pAAm ($R_{rm} = -0.59$, $p < 0.001$). Collectively, the findings from this study indicate that intra-articular viscosupplement injections are not evenly distributed inside a joint, and the tribological outcomes of these materials is strongly determined by the ability of the material to localize to the articulating surfaces in the joint.

KEY WORDS

biodistribution, cartilage, lubrication, tribology, Viscosupplement

1 | INTRODUCTION

Articular cartilage is a remarkable load-bearing material that exhibits one of the lowest reported coefficients of friction in nature, even over decades of activity.¹ The synovial fluid (SF) in the joint is a viscous, non-Newtonian fluid that lubricates the cartilage, meniscus, and synovium. The lubricating ability of SF is mediated by the action of hyaluronic acid (HA), the viscous component of SF, lubricin (or proteoglycan 4) which

supports boundary mode lubrication, and phospholipids, which support hydration lubrication.^{2–7} The lubricating ability of SF varies widely after injury or inflammation, with several studies reporting an increase in the coefficient of friction, and dramatic changes in the viscoelastic properties like the viscosity of the SF via the breakdown of high molecular weight HA to lower molecular weight HA fragments.^{8–13}

To address this drop in viscosity, intra-articular injections of HA commonly known as viscosupplementation, have been the cornerstone

of arthritis treatments for decades.^{14–17} Viscosupplementation hinges on the idea that the restoration of the viscosity of inflamed or injured SF can restore cartilage lubrication, and thereby restore mechanical function. However, the efficacy and mechanism of action of HA viscosupplementation is poorly understood and widely debated, with several clinical societies offering varying recommendations for its use.^{18–20} HA is also susceptible to enzymatic degradation by hyaluronidase, which can affect the distribution of the injected material within the joint and may play a role in the long term clinical outcomes.^{21–26} Additionally, most commercially available HA viscosupplements have varying chemical structures with wide ranges of molecular weights, crosslinking densities, and chemical modifications.^{27–29} These large differences in chemical structure may be responsible for the wide range of clinical outcomes associated with these products.

Despite being used in the clinic for decades, only a few studies have examined and quantified the distribution of injected HA viscosupplements inside articulating joints. A recent study examined the distribution of an HA-methylene blue mixture inside human cadaveric knee joints after administration, and characterized the aggregation of the mixture at various sites using gross images of the joint.³⁰ Other studies have used chemically modified HA hydrogels in small animal models and showed that the gels were present inside the injected limbs for several days after administration.³¹ However, these studies did not assess the distribution of the viscosupplement within the joint, particularly in identifying whether there are differences in the distribution or aggregation of the injected material at the articulating surfaces or in the surrounding soft tissues of the joint capsule.

While a greater localization of injected viscosupplements at the articulating surface of cartilage could potentially improve mechanical outcomes, the extent to which such intra-articular therapies interact with cartilage is complex, unclear, and vastly understudied. These challenges surrounding the establishment of a clear mechanism of action of viscosupplementation have led to an increased interest in the development of synthetic viscosupplements. These materials are synthetic biocompatible polymers, designed to have a very specific chemical structure with controlled molecular weights and cross-linking densities, and can mimic the structure of native HA or other biolubricants, with added functionality like resistance to enzymatic degradation.^{32–34} Recently, a 4 wt% highly crosslinked viscous polyacrylamide (pAAm) hydrogel viscosupplement was shown to substantially decrease symptoms of lameness in a cohort of 43 horses, up to 2 years after follow up.^{35–37} Additionally, the hydrogel was shown to effectively lubricate healthy and degraded cartilage explants and was characterized as a viscous lubricant.³⁷ Strikingly, the hydrogel was found to adhere to the surface of cartilage explants after friction tests and even survived histological processing. But, several questions remain about the ability of the pAAm hydrogel to interface with the articulating cartilage surfaces inside a live, articulating equine joint. Moreover, understanding the quantitative distribution of these injections within a joint would provide vital insight into the potential mechanism of action of such materials, and could inform the design of viscosupplements that preferentially localize to damaged articulating surfaces in a joint.

While there is some qualitative information about the distribution and coverage of HA inside a joint,^{30,31} there is no information about

the localization of synthetic viscosupplements like pAAm. The goal of this study was to measure the distribution of a fluorescently labeled pAAm hydrogel 48 h after being injected into a live equine metacarpophalangeal or metatarsophalangeal (fetlock) joint (MC/MTIII joint) and determine (1) the extent of localization of the pAAm to the articulating cartilage and surrounding soft tissue surfaces in the fetlock joint, and (2) determine whether preferential localization of pAAm on the cartilage surfaces influences the tribological properties of the tissue.

2 | MATERIALS AND METHODS

2.1 | Experimental design

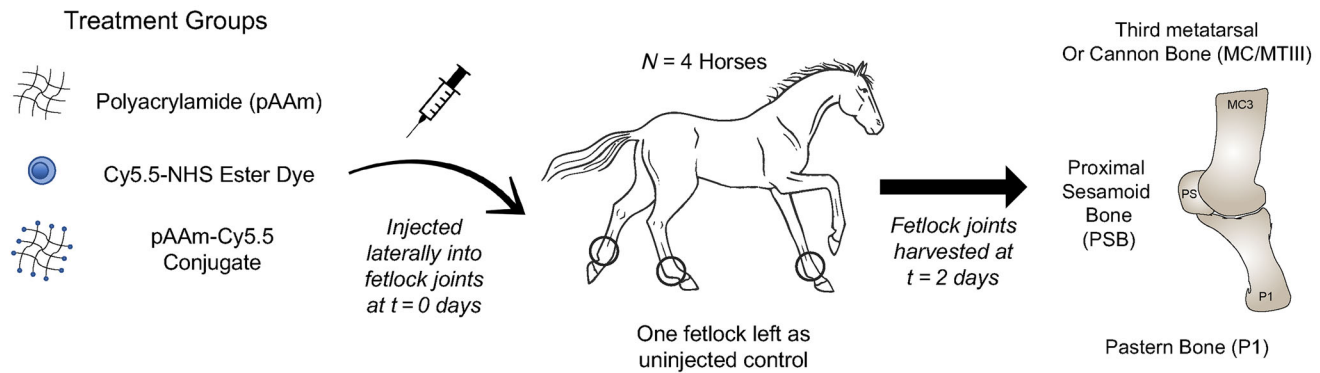
To assess the quantitative distribution of pAAm viscosupplements (NoltrexVet, Nucleus ProVets, Kennesaw, GA) in an equine model, 2.5 mL of a fluorescently labeled (pAAm-Cy5.5, injected in $n = 4$ joints see Supporting Information about dye conjugation protocol), 2.5 mL of a vehicle control unlabeled (pAAm, injected in $n = 4$ joints), and a 2.5 mL of Cy5.5 dye (injected in $n = 2$ joints) at a concentration of 2.7 μ M dissolved in sterile phosphate buffered saline (matched to concentration of dye in the pAAm-Cy5.5 conjugate, see Figure S1 in the Supporting Information) were administered using a lateral approach with the joint in flexion.³⁸ The fetlock joints were administered the assigned treatment in four skeletally mature horses (two geldings and two mares, 13 ± 8 years old) 48 h prior to sacrifice.

Each horse had an uninjected fetlock ($n = 4$ fetlocks) to serve as a control to account for the background tissue fluorescence during fluorescence imaging. The fetlocks in the Cy5.5 dye group ($n = 2$ injected fetlocks) served as positive controls for *in vivo* fluorescence, and were used to confirm the conjugation of the Cy5.5-NHS ester dye to the pAAm hydrogel. After intra-articular administration of the treatment groups, all horses were euthanized for reasons unrelated to this study using the AVMA approved method of euthanasia with a barbiturate overdose (additional information about the horses can be found in Table S1). Intact fetlock joints from each limb were harvested immediately after euthanasia, and dissected after 24 h to image the cartilage and surrounding soft tissue regions lining the cannon bone (third metacarpal/metatarsal bone, MC/MTIII), the short pastern bone (proximal phalanx, P1), and the proximal sesamoid bones (PSB) as shown in Figure 1.

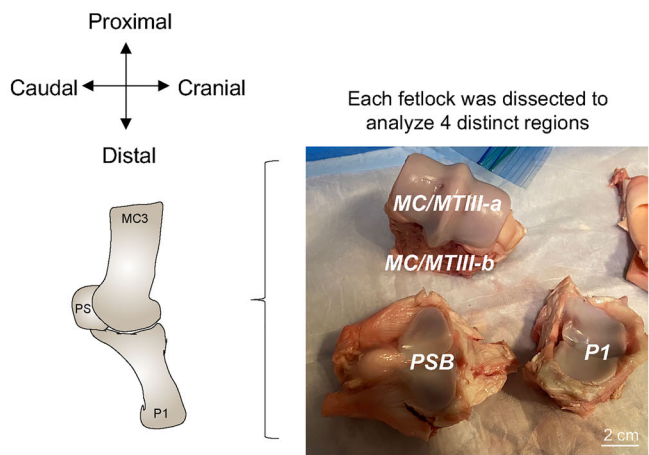
3 | IVIS IMAGING

All four sections of each fetlock were imaged using the *in vivo* imaging (IVIS) Spectrum system (Perkin-Elmer) to determine the fluorescent distribution of each treatment group on the cartilage and soft tissue regions within the joint. To thoroughly characterize the MC/MTIII section, it was split into the MC/MTIII-a, which is the surface of the phalangeal groove of the cannon bone and is the distal weightbearing surface, and the MC/MTIII-b section, which is the soft tissues at the articulation of the MC/MTIII and PSB regions near the injection site (Figure 1B).

(A) In vivo Study Design



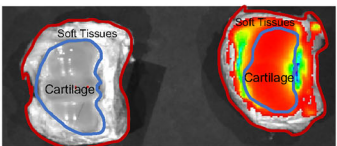
(B) Image Analysis and Outcomes



Planar Fluorescence Imaging (IVIS)

Quantification via area normalized radiant efficiency

- Cartilage (blue ROI)
- Soft Tissues (red ROI)



Tribological Evaluation of Osteochondral Cores

Coefficient of Friction measured in

- Healthy bovine synovial fluid (BSF)
- At 0.1, 1, and 10 mm/s

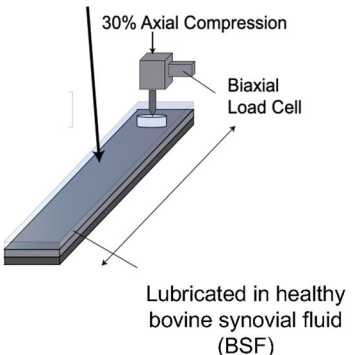


FIGURE 1 (A) Schematic indicating the treatment groups in each fetlock joint in each horse. (B) Overview of the fluorescent imaging and tribological outcomes of the cartilage regions in the fetlock 48 h after polyacrylamide administration.

Each region from each fetlock, from all treatment groups were imaged on the IVIS Spectrum system using the 675–720 nm fluorescence filter pair for the Cy5.5 dye beside the uninjected control section to remove any tissue autofluorescence at this excitation wavelength. While automatically accounted for by the IVIS Living Image software, each photograph and fluorescence overlay image was acquired at a 0.5 s exposure time, medium pixel binning, and the same camera aperture settings to enable comparisons between treatment groups and fetlock sections. Fluorescent intensity was measured in the units of radiant efficiency, a ratio of the emitted to absorbed intensity of the fluorophore and commonly used to measure of the extent of localization or aggregation of fluorescent materials in tissues.^{39,40} Radiant efficiency data was normalized to the area of the

region-of-interest (ROI) to account for differences in sample geometry between fetlocks and horses. After IVIS imaging, each fetlock section was frozen at -20°C in opaque plastic bags for further tribological evaluation and histological analysis.

3.1 | Tissue harvest

3.1.1 | Osteochondral cores

Osteochondral cores (6 mm diameter) were isolated from the cartilage regions lining the MC/MTIII, P1, and PSB regions in the fetlock joint using a drill press (JET Tools) while cooling with room temperature

phosphate buffered saline (MediaTech). All osteochondral cores ($n = 21$ total) were trimmed down to a height of approximately 4 mm and then frozen at -20°C prior to tribological evaluation.

3.2 | Tribological evaluation

Tribological characterization of the osteochondral cores was performed using a previously described, custom cartilage-on-glass tribometer.⁴¹ Frozen osteochondral cores from each region of each fetlock were thawed in PBS with protease inhibitors (Thermo Fisher Scientific) prior to the friction tests. The samples were glued to brass pivots (6 mm diameter), mated against a polished glass surface and tested in healthy bovine synovial fluid (BSF, Lampire Biologics, Pipersville, PA). The cores were then compressed to 30% axial strain (relative to the cartilage thickness) and allowed to stress relax for 1 h. After equilibration, the glass counterface was reciprocated at linear sliding speeds ranging from 0.1–10 mm/s using a DC motor. These compression levels and sliding speeds were chosen based on the strong correlation of the reported friction data to clinical outcomes.²⁷ The coefficient of friction (μ) was recorded as the ratio of shear to normal force measured by a biaxial load cell. All friction coefficients were calculated at the end of sliding when friction reached an equilibrium value and then averaged in the forward and reverse sliding directions to give a mean value for the coefficient of friction at each speed.^{8,37,42,43}

3.3 | Statistical analysis

3.3.1 | IVIS fluorescence data

Fluorescent intensity was quantified using the in vivo imaging system (IVIS) Living Image software (Perkin-Elmer). The ROI tool was used to manually draw areas around the condyles and soft tissues on each fetlock section (example ROIs of cartilage in blue, soft tissues in red are shown in Figure 1B). Fluorescent intensity was calculated in the units of radiant efficiency per unit area which is a ratio of emitted to excited fluorescent light intensity normalized to the surface area of each ROI. The radiant efficiency data was used as a proxy to measure the extent of surface localization of the pAAm-Cy5.5 conjugate. Tissue autofluorescence in each region was accounted for by subtracting the background fluorescent intensity of the uninjected controls in each section and each region. A linear mixed-effects regression model was used to fit $\ln(\text{radiant efficiency})$ as a function of the treatment, region, and age of each horse. Random effects in the model included the fetlock region, nested within each horse. Post-hoc pairwise comparisons (Student's t -test adjusted for multiple comparisons between groups) were conducted to estimate the difference in marginal means of the area-averaged radiant efficiency of the cartilage and soft tissues in each treatment group within each region of the fetlock. Statistical significance was evaluated at $p < 0.05$ using RStudio (version 4.3.2).

3.3.2 | Tribology data

A linear mixed-effects regression model was used to fit coefficient of friction as a function of the sliding speed, treatment, and region. Random effects in the model included the fetlock and limb, nested within each horse. Post-hoc pairwise comparisons (Student's t -tests) were conducted to estimate the difference in marginal means of the coefficient of friction between the pAAm treated and control/Cy5.5 treatment groups. Statistical significance was evaluated at $p < 0.05$. A repeated measures Pearson correlation analysis in conjunction with a linear mixed effects regression model was conducted in RStudio using the rmcrr and lme4 packages to assess the relationship between the measured fluorescent radiant efficiency and coefficient of friction of the cores, with the articulation speeds used as the repeated measure in the analysis.

4 | RESULTS

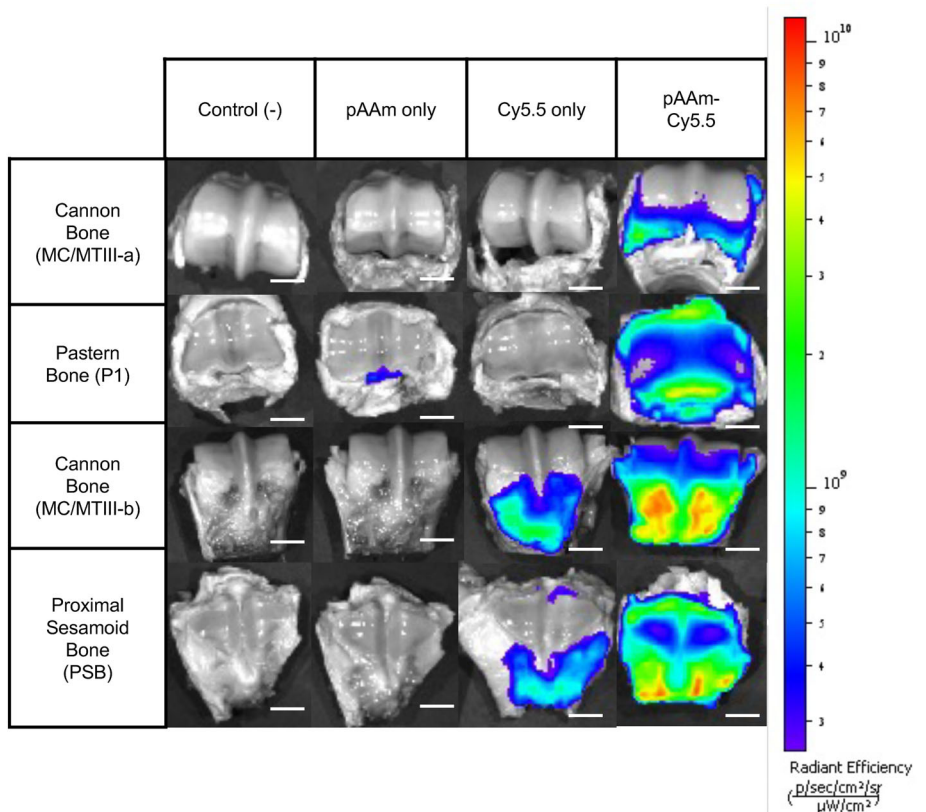
4.1 | Planar fluorescent imaging

To determine the distribution of the fluorescently labeled pAAm hydrogel on the various surfaces within the fetlock following intra-articular administration, 2D planar fluorescence imaging was conducted on all regions from all fetlocks ($n = 14$ total fetlocks, 4 regions per fetlock). Even 2 days post intra-articular administration, the regions closest to the site of the injection exhibited a greater proportion of the injected material (Figure 2, indicated by the red on the heatmap), and the distribution of the injected pAAm hydrogel on the various surfaces of the fetlock joint was not uniform.

The fluorescently labeled (pAAm-Cy5.5) was consistently present on all 4 sections of each fetlock and had higher area-normalized fluorescent intensities compared to the other treatment groups, with radiant efficiencies ranging from 0.5 to $5 \times 10^9 \text{ p/s/sr/cm}^2/\mu\text{W/cm}^2$ for the cartilage and surrounding soft tissue regions (Figure 3A,B). While the Cy5.5 injected fetlocks exhibited moderate fluorescence especially at the articulation of the MC/MTIII-b and PSB regions, the distribution was limited to the soft tissue and synovium in the synovial pouch (Figure 2, rows 3, and 4), with most of the dye being cleared within 48 h.

Unsurprisingly, the uninjected control fetlocks and the unlabeled pAAm injected fetlocks exhibited the lowest fluorescent intensities across all three regions, with baseline area normalized radiant efficiencies ranging from 0.4 to $1 \times 10^8 \text{ p/s/sr/cm}^2/(\mu\text{W/cm}^2)$, two orders of magnitude lower than the Cy5.5 or pAAm-Cy5.5 groups (Figure 3A,B). In contrast, the positive control Cy5.5 treated fetlocks exhibited moderate fluorescent intensities in the synovium regions at the articulation of the PSB and MC/MTIII-b regions, with radiant efficiencies ranging from 2 to $5 \times 10^8 \text{ p/s/sr/cm}^2/(\mu\text{W/cm}^2)$ as shown in Figure 3A. However, the fluorescent intensity of the Cy5.5 group was near baseline levels similar to the uninjected control group in the MC/MTIII-a and P1 regions.

FIGURE 2 Representative IVIS Spectrum fluorescence images of the MC/MTIII, P1, and proximal sesamoid bones sections of the fetlock joints 48 h after injection. Fluorescence (log scale) is quantified as the area normalized radiant efficiency to account for anatomical differences between regions, limbs and horses. Scale bar = 2 cm.



Notably, the fluorescently labeled pAAm hydrogel was not uniformly distributed on the cartilage or soft tissue regions within the fetlock 48 h after administration. The fluorescent intensity of the pAAm-Cy5.5 group on the cartilage regions were consistently three to fourfold higher than the uninjected control and vehicle control pAAm group within each fetlock region (Figure 3A, $p < 0.05$). The highest radiant efficiency of the pAAm-Cy5.5 group was in the soft tissues at the articulation of the MC/MTIII-b and PSB regions, approximately fourfold higher than the pAAm-Cy5.5 intensity in the MC/MTIII-a and P1 regions (Figures 3 and 4A).

To remove the influence of tissue autofluorescence (background signal) on the acquired planar fluorescence data, the average area normalized radiant efficiency of cartilage and soft tissue ROIs from the uninjected control group was subtracted from the radiant efficiency data for all the treatment groups (Figure 3B). After subtraction, the vehicle control pAAm group had no fluorescence since the baseline radiant efficiencies for this group was within 10% of the uninjected control group (Figure 3A). With the exception of the soft tissues in the MC/MTIII-a region, the fluorescent intensities of the pAAm-Cy5.5 treated fetlocks were consistently 2–6 times higher than the Cy5.5 injected fetlocks on both the cartilage and soft tissue regions (Figure 3B, $B > A$, $p < 0.05$). As expected, a greater amount of the pAAm-Cy5.5 conjugate was present in the soft tissue and synovium regions at the articulation of the PSB and MC/MTIII-b regions, near the site of the injection. This difference in background corrected radiant efficiency between the pAAm-Cy5.5 and Cy5.5 treated fetlocks

was observed on the cartilage and surrounding soft tissues in all regions of the fetlock (Figure 3B).

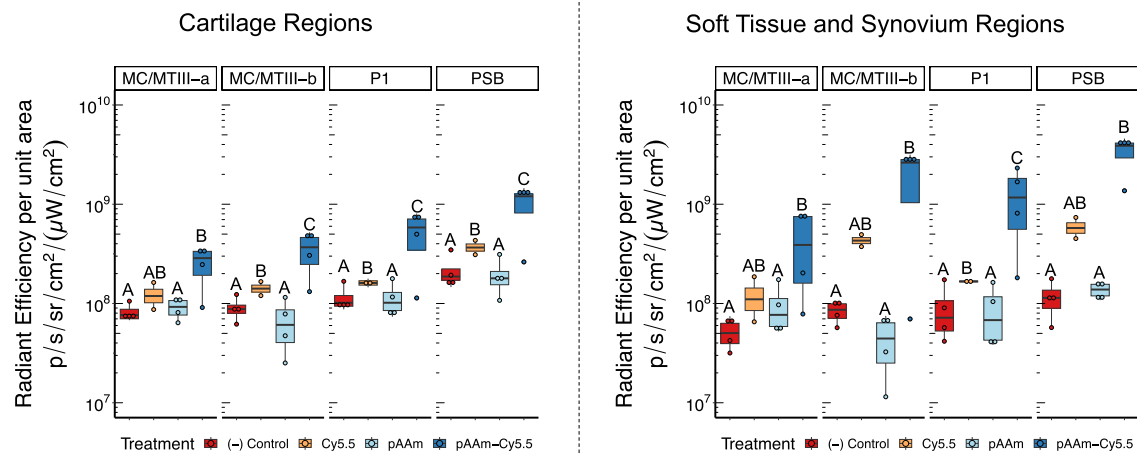
4.2 | Tribological characterization of osteochondral cores

To assess whether localization of pAAm on the cartilage surface could have a functional impact, the ex vivo frictional properties of the osteochondral cores from all regions were measured on a custom cartilage-on-glass tribometer.⁴¹ Tribological evaluation revealed distinct regional differences in friction coefficient between the controls (uninjected and Cy5.5) and pAAm treated (pAAm and pAAm-Cy5.5 fetlocks) joints when lubricated in healthy BSF.

There were no differences in the measured coefficients of friction of the osteochondral cores extracted from the MC/MTIII, P1, and PSB regions from the control fetlock groups (Figure 4A–C, n.s) with friction ranging from $\mu_{avg} = 0.07$ –0.09 across two orders of magnitude of sliding speed from all three regions. These measured coefficients of friction are within 10% of the friction coefficients of neonatal bovine articular cartilage lubricated by BSF in this system.^{2,3,43}

In contrast, the friction coefficients of the pAAm and pAAm-Cy5.5 treated fetlocks varied by region, with the P1 and PSB regions exhibiting lower friction than the MC/MTIII regions depending on the articulation speed. At lower sliding speeds (0.1 and 1 mm/s), the friction coefficients of the osteochondral cores from the P1 ($\mu_{avg} = 0.07$)

(A) Raw IVIS Spectrum Fluorescence Data



(B) Background Subtracted Fluorescence Data

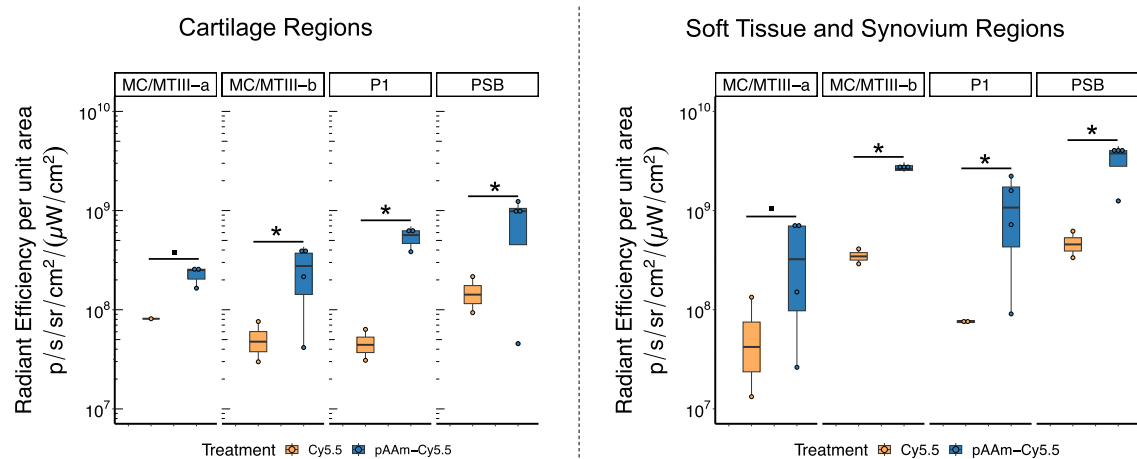


FIGURE 3 (A) Raw IVIS radiant efficiency data of the cartilage and soft tissues from all four treatment groups in each region in each fetlock ($n = 4$ per treatment except $n = 2$ for the Cy5.5 group, per region). Data represents the median radiant efficiency and the range. Statistical comparisons were conducted between treatments within each region. Shared letters denote no statistically significant differences in area normalized radiant efficiency between groups. (B) Background subtraction of tissue autofluorescence revealed the pAAm-Cy5.5 conjugate exhibited significantly higher fluorescence compared to the Cy5.5 only injection group in all four regions of the fetlock, except the MC/MTIII-a soft tissue region. Highest signal strength was observed at the site of injection (at the articulation of the P1 and proximal sesamoid bones).

and PSB ($\mu_{avg} = 0.06$) regions were around 45%–50% lower than the MC/MTIII ($\mu_{avg} = 0.12$) regions (Figure 4A,B, $p < 0.05$), with no statistically significant difference between the P1 and PSB regions. At higher sliding speeds (10 mm/s), the coefficient of friction of the P1 region ($\mu_{avg} = 0.05$) was around 50% lower than the MC/MTIII region ($\mu_{avg} = 0.1$) (Figure 4C, $p < 0.01$), and around 37% lower than the PSB region ($\mu_{avg} = 0.08$) (Figure 4C, $p < 0.05$). While the coefficient of friction of the PSB region was approximately 20% lower than the MC/MTIII region, this difference was not statistically significant (Figure 4C, $p > 0.05$). The osteochondral cores from the MC/MTIII regions in the pAAm fetlocks exhibited slightly higher friction coefficients than the MC/MTIII regions from the control fetlocks across all sliding speeds (Figure 4A–C) however this difference was not statistically significant ($p > 0.1$).

Collectively, these data show that fetlocks injected with the pAAm exhibit regional differences in frictional properties, and these differences can be explained by the varying degrees of localization on the articulating surfaces within the fetlock. Specifically, the P1 and PSB regions had a greater amount of pAAm gel on the surface, and improved tribological outcomes relative to the MC/MTIII regions.

4.3 | Repeated measures correlation analysis

To understand the functional implications of lubricant localization on the cartilage surfaces *in vivo*, a repeated measures Pearson correlation analysis was conducted on a sample-by-sample basis between the coefficients of friction measured at 0.1, 1, and

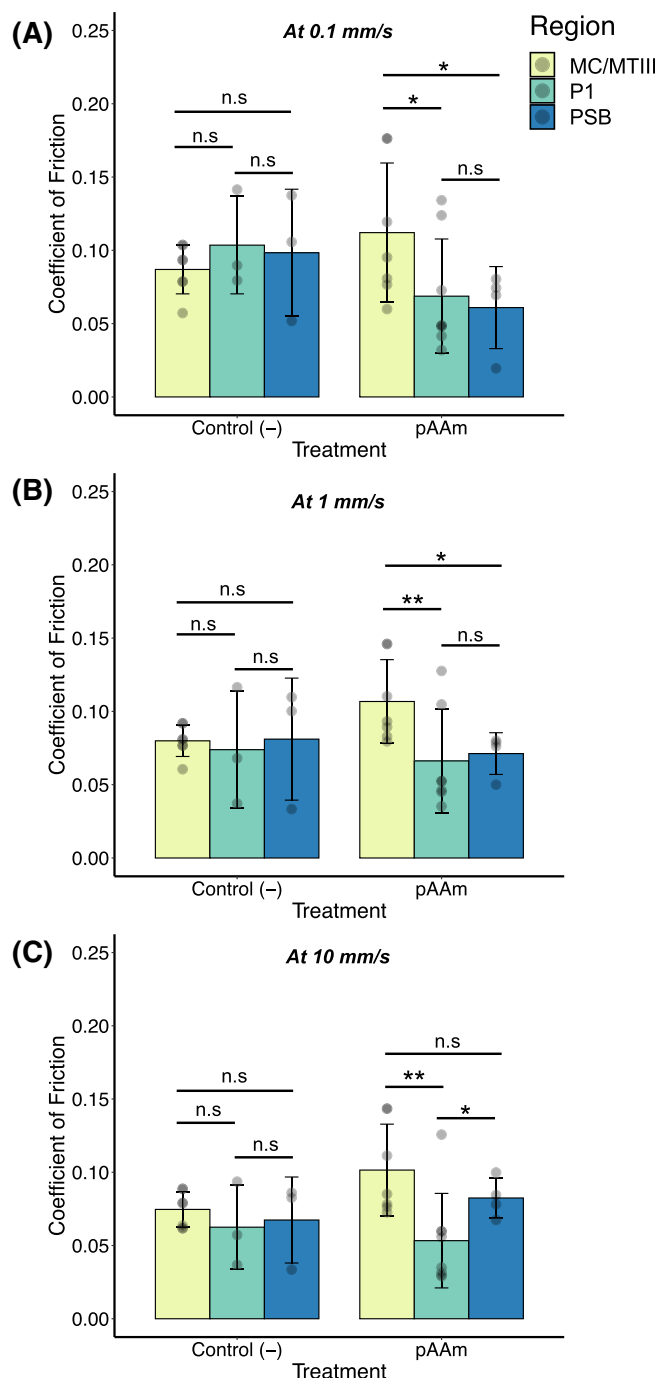


FIGURE 4 Measured coefficients of friction of osteochondral cores extracted from the MC/MTIII, P1, and proximal sesamoid bones regions ($n = 21$ total) evaluated at (A) 0.1, (B) 1, and (C) 10 mm/s in healthy bovine synovial fluid. Data represents the mean \pm standard deviation. Statistically significant differences in the mean friction coefficients are represented using asterisks. Significance was evaluated at $p < 0.05$.

10 mm/s, and fluorescent radiant efficiency of the cartilage from the MC/MTIII-a, P1, and PSB regions from the pAAm-Cy5.5, Cy5.5 only, and control uninjected fetlocks. The pAAm only treated fetlocks were excluded from this analysis since we expect no

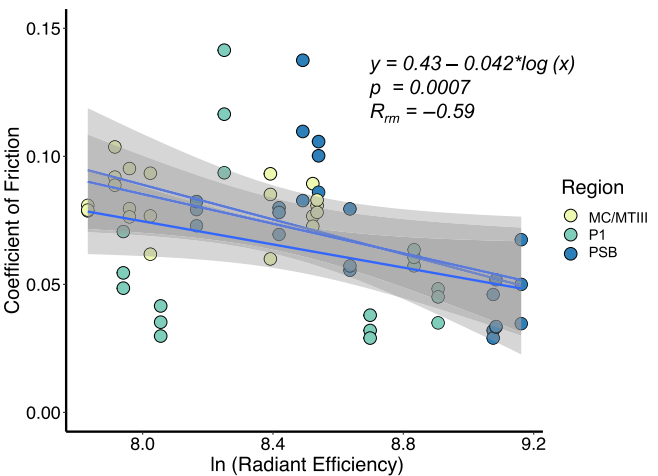


FIGURE 5 A combined mixed effect regression and repeated measured Pearson correlation analysis between the measured coefficient of friction and the radiant efficiency of the cartilage from all regions within the fetlock. Solid lines represent repeated measures linear correlations at 0.1, 1, and 10 mm/s.

correlation between a label-free cartilage lubricant and fluorescent radiant efficiency.

Overall, the repeated measures Pearson correlation analysis revealed a moderately negative and statistically significant correlation between the measured friction and fluorescent radiant efficiency ($R_{rm} = -0.59$, $p < 0.001$, Figure 5). Osteochondral cores extracted from cartilage regions that had a greater fluorescent radiant efficiency (greater than 5×10^8 p/s/sr/cm 2 /(μ W/cm 2)), which was concomitant with a higher amount of material present on the surface (see Figure S1), exhibited lower coefficients of friction of $\mu_{avg} = 0.05$ across two orders of magnitude of sliding speed than those with lowest radiant efficiencies (less than 10^8), with $\mu_{avg} = 0.08$. As observed in Figure 5 friction coefficients of cartilage cores obtained from the P1 and PSB regions of the pAAm-Cy5.5 treated fetlocks exhibited the lowest coefficients of friction when tested across 0.1–10 mm/s in healthy BSF.

Regardless of the treatment, osteochondral cores from the MC/MTIII regions (in yellow) exhibited higher coefficients of friction and low to moderate radiant efficiencies, suggesting that even when pAAm was injected into the fetlock, it is unable to reach the groove of the MC/MTIII bone.

5 | DISCUSSION

The purpose of this study was to develop a method to quantify the distribution of an injectable pAAm viscosupplement 48 h after administration in a large animal joint, and to assess the functional consequence of pAAm localization on cartilage lubrication. Fluorescently labeled pAAm was detected in the joints after 48 h *in vivo*, but the distribution of the material was heterogeneous, with more injected material present in the regions close to the injection site (Figures 2

and 3). In contrast, the positive control dye group had a moderate fluorescent intensity near the injection site, with most of the dye being cleared within 48 h after administration (Figures 2 and 3). Frictional characterization of osteochondral cores revealed regional differences in the coefficient of friction depending on the treatment group (Figure 4). While there were no differences in the friction behavior of osteochondral cores extracted from all regions of the control-treated fetlocks (uninjected or Cy5.5 dye injected), cores extracted from the proximal sesamoid and pastern bones (PSB and P1 regions) of the pAAm-treated fetlocks exhibited significantly lower friction coefficients than cores extracted from the groove of the metacarpal or metatarsal bones (MC/MTIII-a), depending on the articulation speed. Moreover, a repeated measures Pearson correlation analysis between the planar fluorescent intensity and measured coefficient of friction of the cartilage from all regions revealed a moderate and statistically significant correlation between the amount of pAAm present on the cartilage surface and the ex vivo tribological outcomes of the tissue (Figure 5). Collectively, these results indicate that the lubricating efficacy of intra-articularly administered viscosupplements may strongly depend on their ability to localize to the articulating surfaces within a joint *in vivo*.

The heterogenous distribution of injected pAAm in the fetlock is striking. The flexed lateral injection method is a common technique for equine fetlock joints owing to its ease of application, and ability to access the synovial capsule in the fetlock directly. However, the results from our study suggest that viscosupplements injected using conventional techniques may not localize to all articulating surfaces in the joint evenly. This heterogeneity in coverage could be related to injection technique, the relatively short 48 h interval from administration to evaluation, and the amount of pAAm administered. In osteoarthritic equine fetlocks, the cartilage that lines the MC/MTIII, P1, PSB bones can develop osteochondral fragments, wear lines, and erosions, and ultimately leads to subchondral pathology and catastrophic fracture.⁴⁴⁻⁴⁷ To alleviate and prevent these degenerative changes to the joint, viscosupplements are administered to restore the tribological function of the joint and possibly reduce pain, mitigate wear, and ultimately improve the quality of life of the subject/patient.^{28,48,49} However, our data indicates that a majority of the injected material is in the synovial pouch, and only a smaller fraction is present on the cartilage regions closest to the injection site. Notably, the horses in this study did not have any underlying pathology that could affect the distribution of the pAAm gel on the surface of the cartilage in spite of the gel's previously characterized affinity for damaged cartilage surfaces.³⁷ In summary, this finding suggests that the injection route and joint orientation could strongly affect the coverage of material on the articulating surfaces, and ultimately play a factor in the long term clinical outcomes of this class of viscosupplements.

In this study, the cartilage in the MC/MTIII region had the least amount of fluorescently conjugated pAAm and this can be attributed to differences in biomechanical properties of the canon, pastern and PSB, as well as the limited space at the articulation of these bones within the fetlock. Moreover, since the MC/MTIII groove cartilage is located away from the injection site, gravity could also play a role in

the lack of material coverage on this surface. In contrast, a greater amount of the Cy5.5 dye and pAAm-Cy5.5 conjugate was present in the synovium and synovial capsule. It is well established that intra-articularly injected materials are cleared via the lymph nodes and the vascular system in the synovium and sub-synovial layers.^{40,50-52} Previous studies with this pAAm hydrogel have shown it is present in the synovium even 56 days after administration.³⁶ Additionally, the heterogenous morphology of the synovial membrane could make it an attractive site for aggregation of viscous high molecular weight and heavily crosslinked hydrogels like pAAm immediately after injection.

Intra-articular injections of HA are the gold standard of viscosupplements, and have been used clinically for several decades, with nearly 80 approved formulations of HA available globally.^{14,48,53} Owing to HA's susceptibility to enzymatic degradation, previous studies have evaluated the intra-articular residence time of crosslinked formulations of HA, other macromolecules like fluorescently labeled dextrans, and chondrocyte targeting nanoparticles using the IVIS planar fluorescence imaging technique used in this study.^{31,40,52} However, most of these studies were conducted in small animal models (murine or rodent), and did not directly quantify the presence of these materials on the articulating surfaces within the joint, nor did they assess the associated biomechanical outcomes of these injections. Similarly, a recent study by Xiao et al. examined the macroscale distribution of an HA-methylene blue mixture on the surfaces within human cadaveric knee joints and revealed that injection technique can strongly influence the coverage and distribution of these materials in the joint space.³⁰ To the best of our knowledge, a thorough analysis of site-specific distribution and mechanical characterization of HA or viscosupplements within a large animal joint has not been conducted. In this study, we developed a new method to establish a relationship between the distribution of an intra-articularly administered lubricant on a surface inside a large animal joint 2 days after administration, and the tribological properties of the cartilage from various articulating surfaces in the joint. Using this technique to further study temporal trends in the distribution, localization, and mechanical or functional outcomes of the cartilage associated with HA injections, tribosupplements, and other synthetic lubricants could greatly improve our understanding of the mechanisms of action of these therapies.

A clinically relevant question is whether the heterogeneity in lubricant localization within a joint can influence clinical outcomes overall. Previous work by Xiao et al showed that the coverage of a high molecular weight HA-methylene blue mixture inside cadaveric human knee joints is altered depending on the route of administration.³⁰ Further, the clinical component of the study also revealed that commercially available HA viscosupplements injected via the medial midpatellar injection route yielded greater improvements in clinical outcomes like Western Ontario and McMaster Universities Osteoarthritis Score Index (WOMAC) and pain scores compared to the anteromedial injection route. Collectively, the findings from the Xiao et al. study and the present study indicate that method of injection can strongly influence clinical outcomes, and also alters local tribological properties of the cartilage within the articulating joint. Our previous work characterized the variation in frictional properties of seven

commercially available HA formulations and found a strong relationship between the measured friction coefficient on our custom tribometer system and improvements in patient WOMAC scores²⁷ ($R^2 = 0.7$). Using this relationship, a three-fold drop in the friction coefficient of HA (0.15 to 0.05), was associated with a nearly 25-point improvement in patient WOMAC score, with coefficient of friction accounting for 70% of the variability in WOMAC scores. Putting the data from the present study in the context of this established relationship in our system, it is quite plausible then that a two-fold reduction in the friction could lead to improved clinical outcomes. The data from this study indicates that the articulation regions within a fetlock that had a greater localization of pAAm exhibited a nearly two-fold lower friction than the regions lacking it. This two-fold reduction in friction could imply that the pAAm present in these regions is protecting the cartilage better, and may possibly lead to improved clinical outcomes for these joints. The repeated measures correlation analysis revealed that nearly 36% of the variability in the amount of material on a surface could confidently be explained by the regional differences in the coefficient of friction.

The method of administration on material localization within an articulating joint could have important clinical implications. The data from this study suggest that regardless of the injection site, the majority of the pAAm hydrogel tends to be distributed in the soft tissue regions near the injection site, particularly in the folds that line the synovium. Indeed, the distribution of injected materials inside an articulating joint can strongly depend on the joint's geometry and the anatomical space limitations within the joint. Although the distribution pattern of the fluorescently labeled pAAm hydrogel was heterogeneous, with the PSB and P1 cartilage regions exhibiting more localization than the PSB region, other injection approaches could potentially result in a different distribution, with the injected material migrating dorsally depending on the viscosity of the material and access to the synovial folds. Future studies should evaluate the influence of injection method, joint anatomy, and viscoelasticity of the material when evaluating the in vivo efficacy of an intra-articular viscosupplement.

While our study provides valuable insights into the distribution and mechanical efficacy of the injectable pAAm viscosupplement in equine fetlock joints, it is important to acknowledge the limitation of our small sample size. The cohort of horses utilized in this study was randomly selected, encompassing varying degrees of disease severity, age, and sex. While the relatively small number of subjects may limit the generalizability of our findings, the extensive analysis of distribution and mechanics of the fetlocks from all limbs and horses gives us more insight into regional differences in articulating surfaces within each joint. Future studies with larger sample sizes, more diverse populations of equine subjects, and at later time points are warranted to further validate our results and enhance the robustness of our conclusions. Another limitation is the efficiency of the dye conjugation reaction. The fluorescent labeling reaction of the dye to the pAAm hydrogel occurs post gelation, and not at the synthesis stage of the polymer which can prevent a full characterization of the molar ratio of dye bound to the polymer. However extensive dialysis during the

reaction was able to remove any excess unbound dye making the conjugate stable for in vivo imaging analysis (see Supporting Information). The use of a cartilage-on-glass tribometer system is also a limitation. However, the friction measurements involving equine cartilage on glass in this system are comparable to adult human-on-human and equine-on-equine cartilage, and have been shown to be predictive of changes in clinical outcome WOMAC scores in humans.^{2,3,27,41} It is also important to underscore the context of using the equine fetlock joint model. While not a proxy for the stifle or human knee joint, equine cartilage has similar appearance, thickness, and biomechanical properties to human articular cartilage,^{54–56} making it an appropriate animal model to study the tribological changes after the administration of a viscosupplement.

6 | CONCLUSION

In conclusion, we have shown the pAAm hydrogel localizes to various surfaces within an articulating joint. Two days after administration, the hydrogel was found to be heterogeneously distributed within the joint, with cartilage regions that had more localization exhibiting lower ex vivo coefficients of friction. Collectively, the findings from this study suggest that intra-articular injections are not evenly distributed inside a joint, and the tribological outcomes of these materials is strongly determined by the ability of the material to interface with the articulating surfaces in the joint. These findings could be applied to the development of a new class of viscosupplements; hydrogels that can improve the biomechanical and tribological outcomes of the articular cartilage via the use of cartilage binding strategies, and also potentially serve as drug delivery vehicles that can alter OA inflammatory mechanisms in the fat pad and synovium, to ultimately address and study several disease mechanisms in the different tissues in articulating joints.

AUTHOR CONTRIBUTIONS

K.V. contributed to research design, data acquisition, analysis, and interpretation, as well as the authoring and editing of this manuscript. S.M. contributed to the research design, data analysis, and interpretation, as well as the editing of this manuscript. L.J.B. contributed to research design, analysis, and interpretation, and editing of this manuscript.

ACKNOWLEDGMENTS

The authors would like to acknowledge funding and supply of materials from Nucleus ProVets, LLC. We would also like to thank Tina Abratte, Caroline L. Thompson, Drs. Erica J. Secor, and Machiel Ysaebrecht for their assistance with IVIS imaging, tissue harvest and histological processing. The facilities and instruments used in this study were also supported by Cornell Center for Materials Research, grant number DMR1719875, Cornell University. Imaging data was acquired through the National Institute of Health, with S10OD025049 for the IVIS Spectrum. Funding was also provided by National Science Foundation LEAP-HI CMMI 2245367.

CONFLICT OF INTEREST STATEMENT

Dr. Bonassar is a co-founder of and holds equity in 3DBio Corp. Dr. McClure has served as a scientific consultant for Nucleus ProVets, LLC.

DATA AVAILABILITY STATEMENT

The data that support the findings of this study are available from the corresponding author upon reasonable request.

ORCID

Karan Vishwanath  <https://orcid.org/0000-0003-2910-9176>

REFERENCES

1. McCutchen CW. The frictional properties of animal joints. *Wear*. 1962;5:1-17.
2. Bonnevie ED, Galessio D, Secchieri C, Cohen I, Bonassar LJ. Elastoviscous transitions of articular cartilage reveal a mechanism of synergy between Lubricin and hyaluronic acid. *PLoS One*. 2015;10:e0143415.
3. Gleghorn JP, Jones ARC, Flannery CR, Bonassar LJ. Boundary mode lubrication of articular cartilage by recombinant human lubricin. *J Orthop Res*. 2009;27:771-777.
4. Jay GD, Harris DA, Cha C-J. Boundary lubrication by lubricin is mediated by O-linked β (1-3)gal-GalNAc oligosaccharides. *Glycoconj J*. 2001;18:807-815.
5. Chang PD, Abu-Lail NI, Coles JM, Guilak F, Jay GD, Zauscher S. Friction force microscopy of lubricin and hyaluronic acid between hydrophobic and hydrophilic surfaces. *Soft Matter*. 2009;5:3438-3445.
6. Zappone B, Greene GW, Oroudjev E, Jay GD, Israelachvili JN. Molecular aspects of boundary lubrication by human Lubricin: effect of disulfide bonds and enzymatic digestion. *Langmuir*. 2008;24:1495-1508.
7. Schmidt TA, Gastelum NS, Nguyen QT, Schumacher BL, Sah RL. Boundary lubrication of articular cartilage: role of synovial fluid constituents. *Arthritis Rheum*. 2007;56:882-891.
8. Feeney E, Peal BT, Inglis JE, et al. Temporal changes in synovial fluid composition and elastoviscous lubrication in the equine carpal fracture model. *J Orthop Res*. 2019;37:1071-1079.
9. Kosinska MK, Ludwig TE, Liebisch G, et al. Articular joint lubricants during osteoarthritis and rheumatoid arthritis display altered levels and molecular species. *PLoS One*. 2015;10:e0125192.
10. Antonacci JM, Schmidt TA, Serventi LA, et al. Effects of equine joint injury on boundary lubrication of articular cartilage by synovial fluid: role of hyaluronan. *Arthritis Rheum*. 2012;64:2917-2926.
11. Grissom MJ, Temple-Wong MM, Adams MS, et al. Synovial fluid lubricant properties are transiently deficient after arthroscopic articular cartilage defect repair with platelet-enriched fibrin alone and with mesenchymal stem cells. *Orthop J Sports Med*. 2014;2:232596711454258.
12. Elsaied KA, Jay GD, Warman ML, Rhee DK, Chichester CO. Association of articular cartilage degradation and loss of boundary-lubricating ability of synovial fluid following injury and inflammatory arthritis. *Arthritis Rheum*. 2005;52:1746-1755.
13. Vishwanath K, Secor EJ, Watkins A, Reesink HL, Bonassar LJ. Loss of effective lubricating viscosity is the primary mechanical marker of joint inflammation in equine synovitis. *J Orthop Res*. 2024;42:1438-1447. doi:10.1002/jor.25793
14. Balazs EA, Denlinger JL. Viscosupplementation: a new concept in the treatment of osteoarthritis. *J Rheumatol*. 1993;20:3-9.
15. Swann DA, Radin EL, Nazimiec M, Weisser PA, Curran N, Lewinnek G. Role of hyaluronic acid in joint lubrication. *Ann Rheum Dis*. 1974;33:318-326.
16. Strauss EJ, Hart JA, Miller MD, Altman RD, Rosen JE. Hyaluronic acid Viscosupplementation and osteoarthritis: current uses and future directions. *Am J Sports Med*. 2009;37:1636-1644.
17. Moskowitz RW. Hyaluronic acid supplementation. *Curr Rheumatol Rep*. 2000;2:466-471.
18. Jevsevar DS. Treatment of osteoarthritis of the knee: evidence-based guideline, 2nd edition. *JAAOS-J Am Acad Orthop Surg*. 2013;21(9):571-576.
19. Trojan TH, Concoff AL, Joy SM, Hatzenbuehler JR, Saulsberry WJ, Coleman CI. AMSSM scientific Statement concerning Viscosupplementation injections for knee osteoarthritis: importance for individual patient outcomes. *Clin J Sport Med off J Can Acad Sport Med*. 2016;26:1-11.
20. Hochberg MC, Altman RD, April KT, et al. American College of Rheumatology 2012 recommendations for the use of nonpharmacologic and pharmacologic therapies in osteoarthritis of the hand, hip, and knee. *Arthritis Care Res*. 2012;64:465-474.
21. Gupta RC, Lall R, Srivastava A, Sinha A. Hyaluronic acid: molecular mechanisms and therapeutic trajectory. *Front Vet Sci*. 2019;6:192.
22. Watkins A, Fasanella D, Stefanovski D, et al. Investigation of synovial fluid lubricants and inflammatory cytokines in the horse: a comparison of recombinant equine interleukin 1 beta-induced synovitis and joint lavage models. *BMC Vet Res*. 2021;17:189.
23. Tamer TM. Hyaluronan and synovial joint: function, distribution and healing. *Interdiscip Toxicol*. 2013;6:111-125.
24. Hummer CD, Angst F, Ngai W, et al. High molecular weight Intraarticular hyaluronic acid for the treatment of knee osteoarthritis: a network meta-analysis. *BMC Musculoskelet Disord*. 2020;21:702.
25. Band PA, Heeter J, Wisniewski HG, et al. Hyaluronan molecular weight distribution is associated with the risk of knee osteoarthritis progression. *Osteoarthr Cartil OARS Osteoarthr Res Soc*. 2015;23:70-76.
26. Kikuchi T, Yamada H, Shimmei M. Effect of high molecular weight hyaluronan on cartilage degeneration in a rabbit model of osteoarthritis. *Osteoarthr Cartil*. 1996;4:99-110.
27. Bonnevie ED, Galessio D, Secchieri C, Bonassar LJ. Frictional characterization of injectable hyaluronic acids is more predictive of clinical outcomes than traditional rheological or viscoelastic characterization. *PLoS One*. 2019;14:e0216702.
28. Peck J, Slovok A, Miro P, et al. A comprehensive review of Viscosupplementation in osteoarthritis of the knee. *Orthop. Rev*. 2021;10:69-80.
29. Bellamy N, Campbell J, Welch V, et al. Viscosupplementation for the treatment of osteoarthritis of the knee. *Cochrane Database Syst Rev*. 2006;CD005321:CD005321. doi:10.1002/14651858.CD005321.pub2
30. Xiao J, Hu Y, Huang L, et al. Injection route affects intra-articular hyaluronic acid distribution and clinical outcome in viscosupplementation treatment for knee osteoarthritis: a combined cadaver study and randomized clinical trial. *Drug Deliv Transl Res*. 2021;11:279-291.
31. Gilpin A, Zeng Y, Hoque J, et al. Self-healing of hyaluronic acid to improve in vivo retention and function. *Adv Healthc Mater*. 2021;10:2100777.
32. Wathier M, Lakin BA, Cooper BG, et al. A synthetic polymeric biolubricant imparts chondroprotection in a rat meniscal tear model. *Biomaterials*. 2018;182:13-20.
33. Lakin BA, Cooper BG, Zakaria L, et al. A synthetic bottle-brush poly-electrolyte reduces friction and Wear of intact and previously worn cartilage. *ACS Biomater Sci Eng*. 2019;5:3060-3067.
34. Cooper BG, Bordeianu C, Nazarian A, Snyder BD, Grinstaff MW. Active agents, biomaterials, and technologies to improve biolubrication and strengthen soft tissues. *Biomaterials*. 2018;181:210-226.
35. McClure SR, Wang C. A preliminary field trial evaluating the efficacy of 4% polyacrylamide hydrogel in horses with osteoarthritis. *J Equine Vet*. 2017;54:98-102.

36. McClure SR, Yaeger M, Wang C. Clinical and histologic evaluation of polyacrylamide gel in Normal equine metacarpal /metatarsal-phalangeal joints. *J Equine Vet*. 2017;54:70-77.

37. Vishwanath K, McClure SR, Bonassar LJ. Polyacrylamide hydrogel lubricates cartilage after biochemical degradation and mechanical injury. *J Orthop Res*. 2023;41:63-71.

38. Misheff MM, Stover SM. A comparison of two techniques for arthrocentesis of the equine metacarpophalangeal joint. *Equine Vet J*. 1991; 23:273-276.

39. Cho H, Pinkhassik E, David V, Stuart JM, Hasty KA. Detection of early cartilage damage using targeted nanosomes in a post-traumatic osteoarthritis mouse model. *Nanomedicine Nanotechnol Biol Med*. 2015; 11:939-946.

40. Brown SB, Wang L, Jungels RR, Sharma B. Effects of cartilage-targeting moieties on nanoparticle biodistribution in healthy and osteoarthritic joints. *Acta Biomater*. 2020;101:469-483.

41. Gleghorn JP, Bonassar LJ. Lubrication mode analysis of articular cartilage using Stribeck surfaces. *J Biomech*. 2008;41:1910-1918.

42. Feeney E, Galessio D, Secchieri C, Oliviero F, Ramonda R, Bonassar LJ. Inflammatory and noninflammatory synovial fluids exhibit new and distinct Tribological Endotypes. *J Biomech Eng*. 2020; 142(11):111001-111012.

43. Trujillo RJ, Tam AT, Bonassar LJ, Putnam D. Effective viscous lubrication of cartilage with low viscosity microgels. *Materialia*. 2024;33:102000.

44. Oikawa M, Yoshihara T, Kaneko M. Age-related changes in articular cartilage thickness of the third metacarpal bone in the thoroughbred. *Jpn J Vet Sci*. 1989;51:839-842.

45. Bramlage LR. Part I: operative orthopedics of the fetlock joint of the horse: traumatic and developmental diseases of the equine fetlock joint.

46. Firth EC. The response of bone, articular cartilage and tendon to exercise in the horse. *J Anat*. 2006;208:513-526.

47. Firth EC, Hartman W. An in vitro study on joint fitting and cartilage thickness in the radiocarpal joint of foals. *Res Vet Sci*. 1983;34: 320-326.

48. Pereira TV, Jüni P, Saadat P, et al. Viscosupplementation for knee osteoarthritis: systematic review and meta-analysis. *BMJ*. 2022;378: e069722.

49. Wu Y-Z, Huang HT, Ho CJ, et al. Molecular weight of hyaluronic acid has major influence on its efficacy and safety for Viscosupplementation in hip osteoarthritis: a systematic review and meta-analysis. *Cartilage*. 2021;13:169S-184S.

50. Evans CH, Kraus VB, Setton LA. Progress in intra-articular therapy. *Nat Rev Rheumatol*. 2014;10:11-22.

51. Larsen NE, Dursema HD, Pollak CT, Skrabut EM. Clearance kinetics of a hyalur-based viscosupplement after intra-articular and intravenous administration in animal models. *J Biomed Mater Res B Appl Biomater*. 2012;100B:457-462.

52. Mwangi TK et al. Intra-articular CLEARANCE of labeled DEXTRANS from naive and arthritic rat knee joints. *J Control Release off J Control Release Soc*. 2018;283:76-83.

53. Gonçalves C, Carvalho DN, Silva TH, Reis RL, Oliveira JM. Engineering of Viscosupplement biomaterials for treatment of osteoarthritis: a comprehensive review. *Adv Eng Mater*. 2022;24:2101541.

54. McIlwraith CW, Frisbie DD, Kawcak CE. The horse as a model of naturally occurring osteoarthritis. *Bone Jt Res*. 2012;1:297-309.

55. Kuyinu EL, Narayanan G, Nair LS, Laurencin CT. Animal models of osteoarthritis: classification, update, and measurement of outcomes. *J Orthop Surg*. 2016;11:19.

56. Zaki S, Blaker CL, Little CB. OA foundations-experimental models of osteoarthritis. *Osteoarthr Cartil*. 2022;30:357-380.

SUPPORTING INFORMATION

Additional supporting information can be found online in the Supporting Information section at the end of this article.

How to cite this article: Vishwanath K, McClure SR, Bonassar LJ. Heterogeneous distribution of viscosupplements in vivo is correlated to ex vivo frictional properties of equine cartilage. *J Biomed Mater Res*. 2024;1-11. doi:[10.1002/jbm.a.37766](https://doi.org/10.1002/jbm.a.37766)